Available online at www.sciencedirect.com
ScienceDirect
Physica C 450 (2006) 118–123
PHYSICA C
www.elsevier.com/locate/physc

Phase slips in a one-dimensional superconducting wire: Crossover from quantum tunneling to thermal hopping

Zuli Xu [a], Tiezheng Qian [b,*], Ping Sheng [a]

[a] Department of Physics, The Hong Kong University of Science and Technology, Clear Water Bay, Kowloon, Hong Kong, China
[b] Department of Mathematics, The Hong Kong University of Science and Technology, Clear Water Bay, Kowloon, Hong Kong, China

Received 24 July 2006; accepted 7 September 2006
Available online 19 October 2006

Abstract

We carry out quantum Monte Carlo simulations for the finite temperature behavior of a chain of coupled superconducting grains, whose $T = 0$ characteristics have been presented by Matveev et al. [K.A. Matveev, A.I. Larkin, L.I. Glazman, Phys. Rev. Lett. 89 (2002) 096802]. Quantum phase slips at low temperatures and the crossover to thermal hopping at elevated temperatures are observed. The effect of phase slips on persistent currents is numerically demonstrated.

PACS: 74.40.+k; 73.23.Ra; 73.63.Nm

Keywords: Phase slip; Persistent current; Nanowire

1. Introduction

Recent experiments on superconducting nanowires [1,2] have attracted renewed attention on the electrical and magnetic manifestations of thermal and quantum fluctuations [3], in particular those involving quantum phase slips [4–7]. In general, phase slips occur via thermally activated barrier crossing at temperatures not too far below the bulk critical temperature [8–11], but barrier tunneling becomes the dominant phase slip mechanism when the temperature approaches zero [4–7]. The latter type of fluctuations arises from the number-phase uncertainty relation [12], basic to the understanding of superconductivity in small systems [13]. While theoretical modeling of quantum phase slip (QPS) is complicated, its effect on the ground-state properties of nanowires can be studied by using the simplified model of a chain of coupled superconducting grains as proposed by Matveev, Larkin and Glazman (MLG) [14]. Predictions on the $T = 0$ persistent current have been obtained by using the analytical instanton technique [15,16]. Here we report the results of a numerical study on the MLG model using quantum Monte Carlo simulations [17,18], with the aim of studying quantum phase slips at low temperatures and the crossover from quantum tunneling to thermal hopping at finite temperatures.

2. Model

Consider a chain of N coupled superconducting grains modeled by the Hamiltonian [14]:

$$H = \sum_{n=1}^{N} \left\{ -\frac{E_C}{2} \frac{\partial^2}{\partial \theta_n^2} + E_J \left[1 - \cos\left(\theta_n + \frac{2\pi}{N} \frac{\Phi}{\Phi_0} \right) \right] \right\}. \quad (1)$$

Here the grains are connected by tunneling junctions with Josephson coupling energy E_J, $E_C = (2e)^2/C$ is the charging energy where C is the capacitance of the junction, θ_n is the phase difference across the nth junction, Φ is the magnetic flux enclosed by the closed chain (ring), and Φ_0 is the flux quantum $hc/2e$. In the limit of zero charging energy, the

* Corresponding author. Tel.: +852 23587443; fax: +852 23581643.
E-mail addresses: zlxu@ust.hk (Z. Xu), maqian@ust.hk (T. Qian), sheng@ust.hk (P. Sheng).

0921-4534/$ - see front matter © 2006 Elsevier B.V. All rights reserved.
doi:10.1016/j.physc.2006.09.005

classical minimum-energy states of the chain are obtained by minimizing the potential energy

$$U_J(\{\theta_n\}) = \sum_{n=1}^{N} E_J\left[1 - \cos\left(\theta_n + \frac{2\pi}{N}\frac{\Phi}{\Phi_0}\right)\right] \tag{2}$$

in Hamiltonian (1), with the constraint $\sum_{n=1}^{N}\theta_n = 0$ for the closed chain. It follows that the classical states are given by $\{\theta_n^{(m)}\}$, where m is an integer (the winding number) and $\theta_n^{(m)} = \frac{2\pi m}{N} (\mathrm{mod}\ 2\pi)$, satisfying the constraint $\sum_{n=1}^{N}\theta_n^{(m)} = 0$. (Note that there can be different sets of $\{\theta_n^{(m)}\}$ describing the same physical state.) The corresponding classical energy levels are given by

$$E_m = \frac{2\pi^2 E_J}{N}\left(m + \frac{\Phi}{\Phi_0}\right)^2 \tag{3}$$

for $N \gg 1$. The lowest energy level from Eq. (3) gives the classical ground state energy $E(\Phi)$ (Fig. 1a), from which the zero temperature persistent current $I(\Phi)$ is obtained as $I(\Phi) = c\mathrm{d}E/\mathrm{d}\Phi$, showing a sawtooth behavior (Fig. 1b).

To take into account the quantum fluctuations that occur at finite E_C, we start from the imaginary-time action:

$$S[\{\theta_n(t)\}] = \int_0^{\hbar\beta} \mathrm{d}t \sum_{n=1}^{N} \times \left\{\frac{\hbar^2}{2E_C}\dot{\theta}_n^2(t) + E_J\left[1 - \cos\left(\theta_n(t) + \frac{2\pi}{N}\frac{\Phi}{\Phi_0}\right)\right]\right\}, \tag{4}$$

where $\beta = 1/k_B T$ with k_B being the Boltzmann constant and T the temperature. Equilibrium properties can be obtained by evaluating the partition function

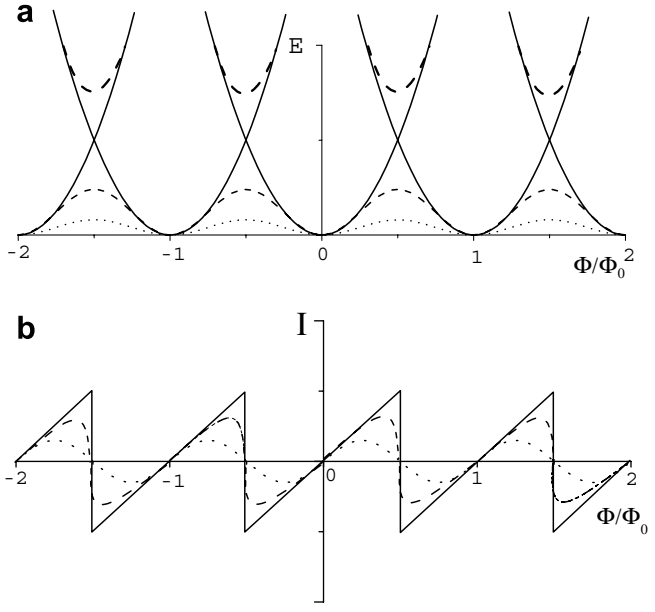

Fig. 1. Schematic illustration of the classical ground state energy $E(\Phi)$ in (a) and the persistent current $I(\Phi) = c\mathrm{d}E/\mathrm{d}\Phi$ in (b). The solid lines denote the case of no quantum fluctuation, the short-dashed lines denote the case of strong quantum fluctuation, and the long-dashed lines denote the case in between.

$$Z(\Phi) = \mathrm{Tr}(\mathrm{e}^{-\beta H}) = \int \prod_{n=1}^{N} D\theta_n(t)\mathrm{e}^{-S/\hbar} \tag{5}$$

subject to the constraints $\sum_{n=1}^{N}\theta_n(t) = 0$ and $\theta_n(0) = \theta_n(\hbar\beta)$, which are the two periodic boundary conditions in space and time. In particular, quantum ground-state properties can be studied in the limit of $\beta \to \infty$. Based on the imaginary-time path-integral expression for Z, quantum fluctuations are manifested through those paths $\{\theta_n(t)\}$ that involve variations of θ_n in imaginary-time. An important class of "large" quantum fluctuations is the QPS, represented by a trajectory of $\{\theta_n\}$ in imaginary-time, starting near one minimum-energy state $\{\theta_n^{(m_1)}\}$ and ending near another state $\{\theta_n^{(m_2)}\}$. Here the change of the winding number (from m_1 to m_2) means that there is a change of the phase at a junction by a multiple of $\pm 2\pi$. Physically, that imaginary-time trajectories of finite action exist between different minima of the potential energy U_J means that there is quantum tunneling between them [15,16]. Based on the action (4), MLG [14] investigated the barrier tunneling effect on quantum ground state energy and persistent current using the instanton technique [15,16]. Their analytical results show that, from the regime of weak tunneling to that of strong tunneling, the shape of the persistent-current oscillations crosses over from sawtooth to sinusoidal behavior and the oscillation amplitude becomes exponentially small (Fig. 1b).

To numerically evaluate the persistent current in the superconducting nanorings modeled by Hamiltonian (1), we use the quantum Monte Carlo simulation which is a powerful numerical method for the study of quantum many-body systems [17,18]. It allows us to explore not only the quantum tunneling regime at low temperature (Section 3) but also the crossover from quantum tunneling to thermal hopping at finite temperature (Section 4). Based on the path-integral expression (5) for the partition function, we compute the persistent current $I(\Phi)$ according to

$$I(\Phi) = c\frac{\mathrm{d}F(\Phi)}{\mathrm{d}\Phi} = \frac{\int \prod_{n=1}^{N} D\theta_n(t)\left[\frac{2eE_J}{\hbar}\frac{1}{N\hbar\beta}\int_0^{\hbar\beta}\mathrm{d}t\sum_{n=1}^{N}\sin\left(\theta_n(t) + \frac{2\pi}{N}\frac{\Phi}{\Phi_0}\right)\right]\mathrm{e}^{-S/\hbar}}{\int \prod_{n=1}^{N} D\theta_n(t)\mathrm{e}^{-S/\hbar}}, \tag{6}$$

where $F(\Phi)$ is the free energy defined by $F(\Phi) = -\beta^{-1}\ln Z(\Phi)$. The Metropolis algorithm [19] is used to generate a Markov chain, which is an ensemble of the $\{\theta_n(t)\}$ configurations distributed according to the probability $Z^{-1}\mathrm{e}^{-S/\hbar}$. For the convenience of numerical calculation, we introduce the dimensionless quantities $\overline{E}_J = \beta E_J$, $\overline{E}_C = \beta E_C$, $\bar{t} = t/\hbar\beta$, $\overline{S} = S/\hbar$, and $\overline{I} = \hbar I/2eE_J$. Accordingly, the dimensionless current may be expressed as

$$\overline{I}(\Phi) = \frac{\int \prod_{n=1}^{N} D\theta_n(\bar{t})\left[\frac{1}{N}\int_0^1 \mathrm{d}\bar{t}\sum_{n=1}^{N}\sin\left(\theta_n(\bar{t}) + \frac{2\pi}{N}\frac{\Phi}{\Phi_0}\right)\right]\mathrm{e}^{-\overline{S}}}{\int \prod_{n=1}^{N} D\theta_n(\bar{t})\mathrm{e}^{-\overline{S}}}, \tag{7}$$

where the dimensionless action is of the form

$$\overline{S} = \int_0^1 \mathrm{d}\bar{t} \sum_{n=1}^{N} \left\{ \frac{1}{2\overline{E}_C} \dot{\theta}_n^2(\bar{t}) + \overline{E}_J \left[1 - \cos\left(\theta_n(\bar{t}) + \frac{2\pi}{N} \frac{\Phi}{\Phi_0} \right) \right] \right\}. \tag{8}$$

Eq. (8) indicates that the equilibrium properties of the system are controlled by the dimensionless parameters $\overline{E}_J$ and $\overline{E}_C$, from which another two dimensionless parameters $\tau = 1/\sqrt{\overline{E}_J \overline{E}_C}$ and $s = \sqrt{\overline{E}_J/\overline{E}_C}$ can be defined.

Physically, τ is the characteristic imaginary-time scale determined from the Lagrangian

$$\overline{L} = \sum_{n=1}^{N} \left\{ \frac{1}{2\overline{E}_C} \dot{\theta}_n^2(\bar{t}) + \overline{E}_J \left[1 - \cos\left(\theta_n(\bar{t}) + \frac{2\pi}{N} \frac{\Phi}{\Phi_0} \right) \right] \right\}$$

in the action $\overline{S}$. For $\tau \ll 1$ (i.e., at sufficiently low temperatures) the instanton, a special trajectory in the course of imaginary-time, displays a phase slip of 2π during a time interval on the order of τ. As for the other parameter s, it is the characteristic action cost associated with a large variation (~ 1) of θ_n over a time interval $\sim\tau$, i.e., $s = 1/\overline{E}_C\tau = \overline{E}_J\tau$.

Consider a ring formed by a large number of junctions ($N \gg 1$), where the QPS occurs at one particular junction [14]. For an instanton trajectory $\{\theta_n(\bar{t})\}$ starting near $\{\theta_n^{(0)}\}$ and ending near $\{\theta_n^{(-1)}\}$, the time variations of θ_n are localized at, say, the kth junction, with $\theta_k(\bar{t}) \approx 4\arctan\{\exp[(\bar{t} - \bar{t}_c)/\tau]\}$, where $\bar{t}_c$ is the phase-slip center in time. That is, in the low-temperature limit $\tau \ll 1$, $\theta_k(\bar{t})$ starts from $\theta_k \approx 0$ for $(\bar{t} - \bar{t}_c)/\tau \to -\infty$ and ends at $\theta_k \approx 2\pi$ for $(\bar{t} - \bar{t}_c)/\tau \to \infty$, describing a phase slip of 2π. The action associated with this instanton trajectory is $\overline{S}_{\mathrm{inst}} = 8s$.

3. Quantum tunneling and persistent current

In this section, we carry out quantum Monte Carlo simulations for low temperatures with the aim of observing rare QPS's with $\tau \ll 1$ and $\overline{S}_{\mathrm{inst}} = 8s > 1$.

An equilibrium ensemble is produced using the Metropolis algorithm. For Φ/Φ_0 close to an integer, most of the configurations $\{\theta_n(\bar{t})\}$ are in the vicinity of the global minimum of $\overline{S}$, i.e., $\{\theta_n(\bar{t}) \approx \theta_n^{(m)}\}$ with weak fluctuations of θ_n in imaginary-time, where m is the integer minimizing $(m + \Phi/\Phi_0)^2$ in the classical energy levels E_m (3). In the case of Φ/Φ_0 near a half-integer, most of the $\{\theta_n(\bar{t})\}$ configurations are in the vicinity of either of the two lowest minima of $\overline{S}$, i.e., $\{\theta_n(\bar{t}) \approx \theta_n^{(m_1)}$ or $\theta_n^{(m_2)}\}$ with weak fluctuations of θ_n in $\bar{t}$, where m_1 and m_2 are the two integers for the two lowest classical energy levels. Quantum phase slips are observed in the rare transitional events that carry the system from one of the minima of $\overline{S}$ to the other. In particular, for Φ/Φ_0 near half-integer, rare transitions are observed mostly between the two lowest minima of $\overline{S}$. Physically, this means that quantum tunneling exists between the two lowest classical energy states $\{\theta_n^{(m_1)}\}$ and $\{\theta_n^{(m_2)}\}$. As a consequence, the E_{m_1} and E_{m_2} degeneracy at half-integer Φ/Φ_0 is broken. The effect of quantum tunneling on ground state energy and persistent current has been discussed by MLG [14] using the instanton technique. Here we present the numerical evidences of the predicted rare transitions.

Fig. 2 shows a sequence of the $\{\theta_n(\bar{t})\}$ configurations. Selected from a segment of the Markov chain, it exhibits a transition from $\{\theta_n(\bar{t}) \approx \theta_n^{(0)}\}$ to $\{\theta_n(\bar{t}) \approx \theta_n^{(-1)}\}$ for $\Phi/\Phi_0 = 0.5$ at which $E_0 = E_{-1}$. It is seen that in the present case of $N \gg 1$, the QPS is indeed nucleated at one junction (the kth junction). First a bubble of $\theta_k \approx 2\pi$ grows out of the background of $\theta_k \approx 0$ through a large fluctuation on the profile of $\theta_k(\bar{t})$. As the Markov chain proceeds, the bubble expands, converting θ_k from ≈ 0 to $\approx 2\pi$ throughout the imaginary-time domain, and the transition from $\theta_k(\bar{t}) \approx 0$ in $\{\theta_n(\bar{t}) \approx \theta_n^{(0)}\}$ to $\theta_k(\bar{t}) \approx 2\pi$ in $\{\theta_n(\bar{t}) \approx \theta_n^{(-1)}\}$ is thus completed. The instanton in imaginary-time, $\theta_k(\bar{t}) = 4\arctan\{\exp[(\bar{t} - \bar{t}_c)/\tau]\}$, is observed as the (left) domain wall, centered at $\bar{t} = \bar{t}_c$ between the domains of $\theta_k \approx 0$ and $\theta_k \approx 2\pi$. Due to the boundary condition $\theta_n(0) = \theta_n(1)$, instanton and anti-instanton must occur together in a trajectory of θ_n in $\bar{t}$ such that $\theta_k(\bar{t})$ varies from ≈ 0 to $\approx 2\pi$ and back to ≈ 0 along the $\bar{t}$ axis (see (c) and (d) in Fig. 2). Since the action associated with an instanton (anti-instanton) is $\overline{S}_{\mathrm{inst}} = 8s$, the $\{\theta_n(\bar{t})\}$ configurations comprising a pair of instanton and anti-instanton appear in the equilibrium ensemble with an exponentially small probability, proportional to e^{-16s}. As a consequence, the Markov chain proceeds by long waiting time around either of the two lowest minima of $\overline{S}$, followed by the rare transitions from one to the other via the QPS mechanism depicted in Fig. 2. In order to simulate an equilibrium ensemble according to the probability $Z^{-1}\mathrm{e}^{-\overline{S}}$, a sufficiently large number of configurations must be generated to include enough rare transition events.

The persistent current is measured according to Eqs. (6) and (7). In order to see the quantum fluctuation effect varying from weak to strong at low temperature, we change $s = \sqrt{\overline{E}_J/\overline{E}_C}$ from large to small while fixing N at 20 and τ at $1/\sqrt{1500}$. That $\tau = k_B T/\sqrt{E_J E_C} \ll 1$ ensures the temperature to be low enough for the quantum fluctuation effect to be important. We will go back to this point in Section 4. In discretizing $\bar{t}$ from 0 to 1, 300 points were used to ensure a good resolution: there are about eight points in an interval of τ. Fig. 3 shows the persistent current $\overline{I}$ as a function of Φ/Φ_0. The quantum fluctuation effect is manifest in the decreased persistent current amplitude with decreasing s parameter value. In particular, the analytical prediction that the shape of the persistent-current oscillations crosses over from sawtooth to sinusoidal behavior [14] is confirmed. The tendency that the current amplitude decreases with the decreasing parameter s may be simply explained as follows.

For Φ/Φ_0 near integer values, the current amplitude is mostly suppressed by the zero-point Gaussian fluctuations around the minimum-energy states $\{\theta_n^{(m)}\}$. This effect can be estimated by considering one junction, in which quantum fluctuations suppress the current amplitude by a factor

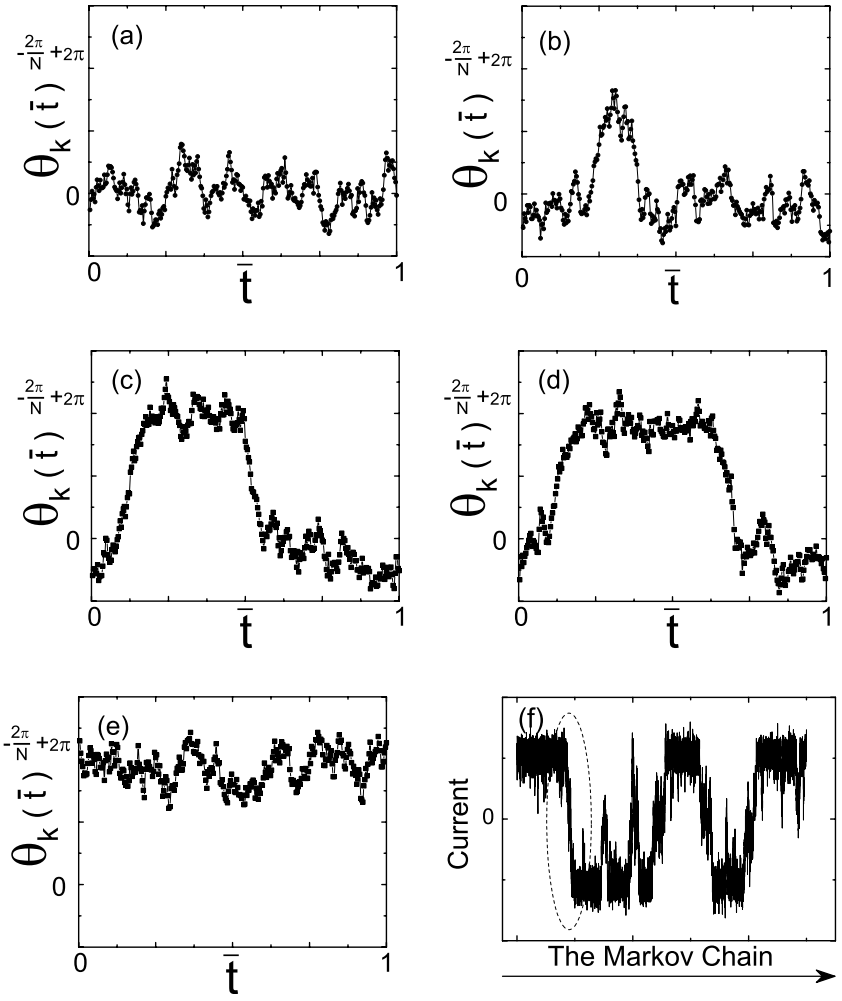

Fig. 2. (a)–(e) The profiles of $\theta_k(\bar{t})$ in a sequence of the $\{\theta_n(\bar{t})\}$ configurations, selected from a segment of the Markov chain for $\Phi/\Phi_0 = 0.5$, $N = 20$, $\overline{E}_J = 30$, and $\overline{E}_C = 60$. They show a transition from $\{\theta_n(\bar{t}) \approx \theta_n^{(0)}\}$ to $\{\theta_n(\bar{t}) \approx \theta_n^{(-1)}\}$ through QPS. The transition proceeds as follows: (a) $\theta_k(\bar{t})$ starts from the vicinity of the minimum $\theta_n^{(0)}$, i.e., $\theta_k(\bar{t}) \approx 0$. (b) A bubble of $\theta_k \approx 2\pi$ grows out of the background of $\theta_k(\bar{t}) \approx 0$ through a large fluctuation. (c) The bubble expands through the two propagating domain walls. (d) The expansion continues and most of the imaginary-time domain has been converted from $\theta_k \approx 0$ to $\theta_k \approx 2\pi$. (e) The transition is completed with $\theta_k(\bar{t})$ ending at the vicinity of the minimum $\theta_n^{(-1)}$, i.e., $\theta_k(\bar{t}) \approx -2\pi/N + 2\pi$. The instanton and anti-instanton are seen as the two propagating domain walls in the two $\theta_k(\bar{t})$ profiles in (c) and (d) in the middle of the sequence. (f) Variation of the persistent current as the Markov chain proceeds. The transition from $\{\theta_n(\bar{t}) \approx \theta_n^{(0)}\}$ to $\{\theta_n(\bar{t}) \approx \theta_n^{(-1)}\}$ exhibits a jump in the current, indicated by the dashed line.

of $\langle \cos\Delta\theta \rangle \approx 1 - \langle (\Delta\theta)^2 \rangle/2$, where $\langle (\Delta\theta)^2 \rangle$ is the square of the uncertainty of the phase, given by $\langle (\Delta\theta)^2 \rangle = 1/s$. It is clear that the $\langle \cos\Delta\theta \rangle$ factor decreases with decreasing s. On the other hand, for Φ/Φ_0 near half-integer values, the current amplitude is mostly suppressed by quantum tunneling between the minimum-energy states $\{\theta_n^{(m_1)}\}$ and $\{\theta_n^{(m_2)}\}$. In this case, the quantum ground state is a superposition of two wave packets, peaked at $\{\theta_n^{(m_1)}\}$ and $\{\theta_n^{(m_2)}\}$ respectively [15,16]. The persistent currents evaluated at these two energy minima are of approximately the same magnitude but opposite in sign. Therefore, the quantum state is a superposition of two persistent-current states of opposite currents [20]. As a consequence, in this state the quantum expectation value of the persistent current must have a magnitude much smaller than that evaluated at either energy minimum, if there is an appreciable degree of quantum superposition that occurs via tunneling. Theoretical analysis based on the instanton technique shows that quantum tunneling effect is exponentially small, controlled by the factor $e^{-\overline{S}_{inst}}$ [14]. In the Monte Carlo simulations here, the tunneling effect is contributed by the $\{\theta_n(\bar{t})\}$ configurations that comprise a pair of instanton and anti-instanton, and these configurations occur in the equilibrium ensemble with an exponentially small probability $\propto e^{-2\overline{S}_{inst}}$. This explains why the persistent current amplitude decreases with the decreasing parameter s for Φ/Φ_0 near half-integer values.

We want to point out that zero temperature can never be reached in quantum Monte Carlo simulations, because $T \to 0$ corresponds to $\tau \to 0$, which requires infinitely many points in discretizing the imaginary-time $\bar{t}$. We therefore have to work with a sufficiently low temperature ($\tau \ll 1$) in order to observe the quantum fluctuation effect on a computationally affordable basis. To demonstrate that

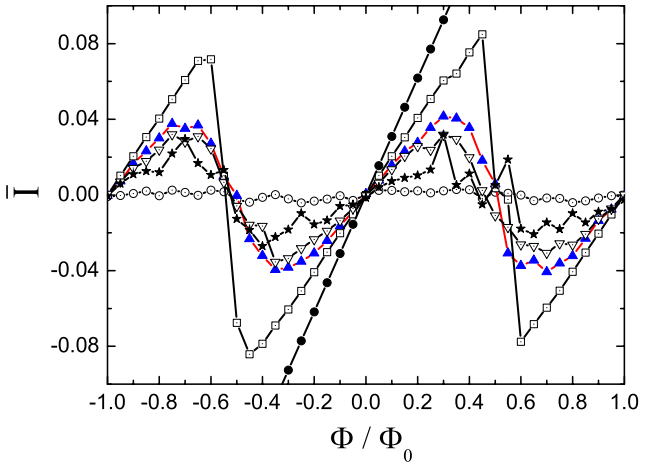

Fig. 3. The persistent current $\bar{I}$ plotted as a function of Φ, evaluated for $N = 20$, with $s = \sqrt{\bar{E}_J/\bar{E}_C}$ varied from large to small, and $\tau = 1/\sqrt{\bar{E}_J\bar{E}_C}$ fixed at $1/\sqrt{1500}$. The squares are for $s = \sqrt{3/5}$, the up-triangles for $s = \sqrt{5/12}$, the down-triangles for $s = \sqrt{48/125}$, the stars for $s = \sqrt{27/80}$, and the empty circles for $s = \sqrt{4/15}$. For comparison, the classical persistent current $\bar{I}_c$ (solid circles) is plotted for $\bar{E}_J$ from 20 to 30. The quantum fluctuation effect on the current amplitude is clearly seen.

quantum effect is indeed manifested in the persistent-current profiles in Fig. 3, we have also carried out Monte Carlo simulations for a classical system governed by the potential energy $U_J(\{\theta_n\})$ in Eq. (2), as a comparison reference. Persistent current in the classical statistical ensemble is measured according to

$$I_c(\Phi) = \frac{\int \prod_{n=1}^{N} d\theta_n \left[\frac{2eE_J}{\hbar}\frac{1}{N}\sum_{n=1}^{N}\sin\left(\theta_n + \frac{2\pi}{N}\frac{\Phi}{\Phi_0}\right)\right] e^{-\beta U_J}}{\int \prod_{n=1}^{N} d\theta_n e^{-\beta U_J}} = \frac{2eE_J}{\hbar}\bar{I}_c(\Phi). \quad (9)$$

Fig. 3 also shows the dimensionless persistent current $\bar{I}_c$ as a function of Φ/Φ_0. For comparison purpose, we use the same values for N and $\bar{E}_J = \beta E_J$ in evaluating $\bar{I}$ according to Eq. (7) and $\bar{I}_c$ according to Eq. (9). It is clearly seen that, compared to $\bar{I}_c$, the amplitude of $\bar{I}$ is appreciably suppressed by quantum fluctuations, and the degree of suppression increases with the decreasing parameter s.

4. Crossover from quantum tunneling to thermal hopping

In Fig. 3 we have varied s with τ fixed at a small value. That is, quantum fluctuations have been tuned at a fixed low temperature. Now, in order to observe the crossover from quantum tunneling to thermal hopping, we increase τ with the value of s fixed. This corresponds to an increase of the temperature. Note that τ is the characteristic imaginary-time span of "large" quantum fluctuations, represented by large variations of $\theta_n(\bar{t})$ in imaginary-time. In particular, τ is the time span of the instanton/anti-instanton structure for QPS. When τ becomes comparable to or larger than 1 which is the total imaginary-time span, large quantum fluctuations are suppressed compared to thermal fluctuations. This can be easily seen by comparing s and $\bar{E}_J = s/\tau$. When τ is much larger than 1, thermal fluctuations with the probability dominated by the factor of $e^{-\bar{E}_J}$ are more probable than quantum fluctuations with the probability dominated by the factor of e^{-s}. Note that $2\bar{E}_J$ is the energy barrier (measured by $k_B T$) for a thermal hopping between two neighboring classical minimum-energy states while $8s$ is the action (measured by $\hbar$) of the instanton/anti-instanton involved in the QPS mechanism for quantum tunneling (Fig. 2).

Fig. 4 shows a sequence of the $\{\theta_n(\bar{t})\}$ configurations. Selected from a segment of the Markov chain, it exhibits a thermal hopping from $\{\theta_n^{(0)}\}$ to $\{\theta_n^{(-1)}\}$ nucleated at the kth junction. It is clearly seen that while quantum fluctuations are still present as evidenced by the small variations of $\theta_k(\bar{t})$ in imaginary time, the transition from $\theta_k(\bar{t}) \approx 0$ to $\theta_k(\bar{t}) \approx 2\pi$ is realized through a change of $\theta_k(\bar{t})$ that is more or less uniform in the imaginary-time domain as the Markov chain proceeds. Compared with Fig. 2, $\theta_k(\bar{t})$ here shows no instanton/anti-instanton structure associated with QPS because large quantum fluctuations are suppressed and thermal hopping becomes the dominant transition mechanism.

We have evaluated the persistent current according to Eqs. (6) and (7) for gradually increased τ with s fixed at $\sqrt{5/12}$ (see Fig. 5). When thermal fluctuations become more and more probable, the amplitude of the persistent current is further suppressed from that obtained in Fig. 3, where quantum fluctuations are dominant.

From these results we conclude that quantum fluctuations become less probable than thermal ones at finite temperatures. The crossover from quantum tunneling to thermal hopping sets in when τ approaches 1, at which the energy barrier scale $\bar{E}_J$ is comparable to the action barrier scale s. This has been confirmed by the direct observa-

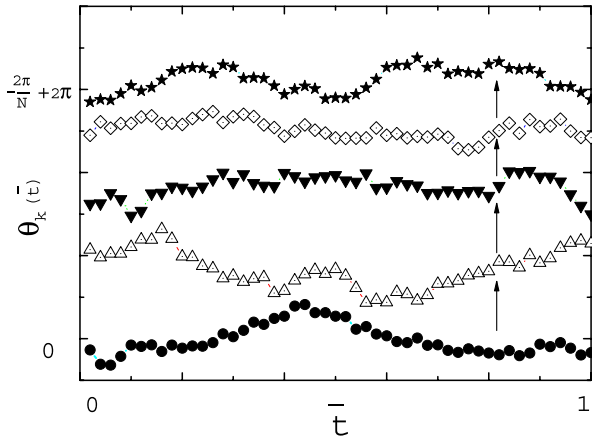

Fig. 4. The profiles of $\theta_k(\bar{t})$ in a sequence of the $\{\theta_n(\bar{t})\}$ configurations, selected from a segment of the Markov chain for $\Phi/\Phi_0 = 0.5$, $N = 20$, $\bar{E}_J = 6.25$, and $\bar{E}_C = 15$. They show a transition from $\{\theta_n(\bar{t}) \approx \theta_n^{(0)}\}$ to $\{\theta_n(\bar{t}) \approx \theta_n^{(-1)}\}$ through thermal hopping (barrier crossing). Compared to Fig. 2, here quantum fluctuations are weak and the transition from $\theta_k(\bar{t}) \approx 0$ to $\theta_k(\bar{t}) \approx 2\pi$ is more or less uniform in the imaginary-time domain as the Markov chain proceeds.

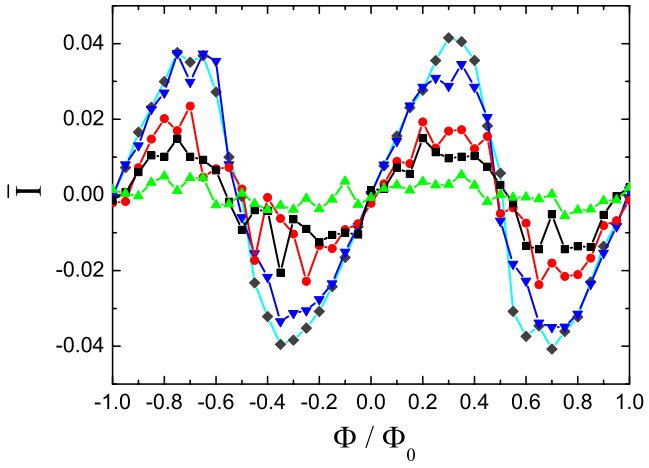

Fig. 5. The persistent current $\bar{I}$ plotted as a function of Φ, evaluated for $N = 20$, with $\tau = 1/\sqrt{\bar{E}_J \bar{E}_C}$ varied from low to high, and $s = \sqrt{\bar{E}_J/\bar{E}_C}$ fixed at $\sqrt{5/12}$. The diamonds are for $\tau = 1/\sqrt{1500}$, the down-triangles for $\tau = 1/\sqrt{375}$, the circles for $\tau = 2/\sqrt{375}$, the squares for $\tau = 1/\sqrt{60}$, and the up-triangles for $\tau = 4/\sqrt{375}$. Compared to Fig. 3, here the current amplitude is further suppressed by the enhanced thermal fluctuations.

tion of thermally activated phase slips through which the transition between neighboring classical energy states is made.

Acknowledgement

This work was supported by Hong Kong RGC Grants HKUST6073/02P, CA04/05.SC02, 602904, and 602805.

References

[1] A. Bezryadin, C.N. Lau, M. Tinkham, Nature (London) 404 (2000) 971.
[2] C.N. Lau, N. Markovic, M. Bockrath, A. Bezryadin, M. Tinkham, Phys. Rev. Lett. 87 (2001) 217003.
[3] W.J. Skocpol, M. Tinkham, Rep. Prog. Phys. 38 (1975) 1049.
[4] N. Giordano, Physica (Amsterdam) 203B (1994) 460, and references therein.
[5] J.M. Duan, Phys. Rev. Lett. 74 (1995) 5128.
[6] Y. Chang, Phys. Rev. B 54 (1996) 9436.
[7] A.D. Zaikin, D.S. Golubev, A. van Otterlo, G.T. Zimanyi, Phys. Rev. Lett. 78 (1997) 1552;
D.S. Golubev, A.D. Zaikin, Phys. Rev. B 64 (2001) 014504.
[8] W.A. Little, Phys. Rev. 156 (1967) 396.
[9] J.S. Langer, V. Ambegaokar, Phys. Rev. 164 (1967) 498.
[10] D.E. McCumber, B.I. Halperin, Phys. Rev. B 1 (1970) 1054.
[11] D.Y. Vodolazov, F.M. Peeters, Phys. Rev. B 66 (2002) 054537.
[12] R.M. Bradley, S. Doniach, Phys. Rev. B 30 (1984) 1138.
[13] M. Tinkham, Introduction to Superconductivity, McGraw-Hill, New York, 1996.
[14] K.A. Matveev, A.I. Larkin, L.I. Glazman, Phys. Rev. Lett. 89 (2002) 096802.
[15] R. Rajaraman, Solitons and Instantons, North-Holland, Amsterdam, 1982.
[16] S. Coleman, Aspects of Symmetry, Cambridge University Press, Cambridge, 1985.
[17] K.E. Schmidt, D.M. Ceperley, in: K. Binder (Ed.), The Monte Carlo Method in Condensed Matter Physics, Springer, Berlin, 1992, p. 203.
[18] H. De Raedt, W. von der Linden, in: K. Binder (Ed.), The Monte Carlo Method in Condensed Matter Physics, Springer, Berlin, 1992, p. 249.
[19] N. Metropolis, A.W. Rosenbluth, M.N. Rosenbluth, A.M. Teller, E. Teller, J. Chem. Phys. 21 (1953) 1087.
[20] C.H. van der Wal et al., Science 290 (2000) 773.